cone-4-Type Calixarenes with Orientable Glycosylthioureido Groups at the Upper Rim: An In-depth Analysis of Their Symmetry Properties

Laura Legnani,[†] Federica Compostella,[‡] Francesco Sansone,[§] Lucio Toma[†]*

[†] *Dipartimento di Chimica, Università di Pavia, Via Taramelli 12, 27100 Pavia, Italy*

[‡] *Dipartimento di Biotecnologie Mediche e Medicina Traslazionale, Università di Milano, Via Saldini 50, 20133 Milano, Italy*

[§] *Dipartimento di Chimica, Università di Parma, Parco Area delle Scienze 17/A, 43124 Parma, Italy*

* Tel: (+39) 0382987843. Fax: (+39) 0382987323. E-mail: lucio.toma@unipv.it

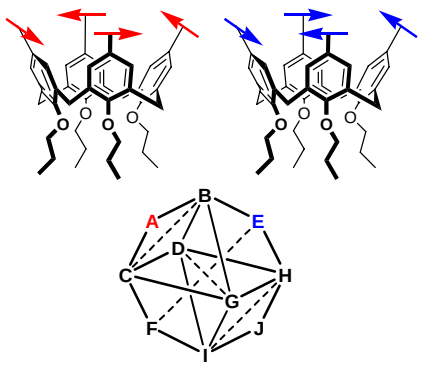

Abstract. The two glycoclusters α- and β-D-mannosylthioureidocalix[4]arenes **1** and **2** in the *cone* geometry have been submitted to a conformational investigation with the DFT approach at the standard B3LYP/6-31G(d) level and using a water continuum solvent model. After a reasoned choice of the level of calculation and the evaluation of the properties of the monomeric components of **1** and **2**, the intrinsic conformational properties of *cone*-calix[4]arenes with orientable groups at the upper rim were thoroughly analyzed. From the possible combinations of the directions that the groups may assume, ten different geometries derive. These geometries are chiral structures interchangeable through two different processes, named *breathing equilibrium* and *arrow rotation*, that allow a dense network connection among them. When the modeling of the whole macrocycles

1 and **2** was performed, a huge difference in their conformational behavior was found that heavily influences the presentation mode of their saccharidic moieties.

Introduction

Multivalent presentation of carbohydrates using suitable conjugation chemistry and scaffold selection may result in a better efficiency and a higher selectivity in the interaction with the corresponding receptors such as lectins and immunoglobulines. The substituents linked to the scaffolds work as fingers that may diverge from the central core or orient themselves parallel to each other and converge toward one or more units of a partner to interact with it. The nature of the scaffolds play a crucial role in the presentation of the substituents as well as the nature of the linkers that connect to them. Calix[*n*]arenes, for example, a well-known class of macrocycles, besides a series of other applications,[1] have been successfully used as scaffolds for multivalent presentation of glycosyl moieties.[2,3] The even-numbered macrocycles (n = 4, 6, 8) have been mostly used. The smallest member in this family of macrocycles (n = 4) has the lowest mobility and, if the alkoxy groups at the lower rim are sufficiently steric demanding, stable conformational isomers exist that allow a controlled display of the saccharide units in the space. Several linkers have been exploited to connect sugars to calixarenes, someone very flexible, someone more rigid.[2,3] In the latter case the linker can heavily constrain the orientation options of the substituents so that their presentation mode may be strongly affected.

In literature, several glycocalix[*n*]arenes have been reported where glycosyl moieties such as glucose, galactose, or lactose are linked as β anomers, through a thiourea unit, to the upper rim of these macrocyclic platforms.[4-10] Despite of, or perhaps thanks to, the proximity of the sugar epitopes to the calixarene cavity, these glycosylthioureidocalixarenes have shown in some cases very interesting inhibition properties towards specific carbohydrate recognition proteins. Together with a high efficiency often associated to a significant multivalent effect, an impressive selectivity has been also observed,[4] for instance in the binding of medically relevant lectins, namely galectins,

belonging to the same family. Interestingly that selectivity resulted strongly related to the size and the geometry of the glycocalixarene. Tetralactosylcalix[4]arenes blocked in the *cone* geometry, *i.e.* that orienting the aryl groups in the same direction, showed[4,5] for example a strong inhibition activity against galectin-3 and no activity against galectin-1.

Another interesting point observed in the previous studies is that a synthetic spacer like thiourea seems, at least in part, to alter the natural specificity of the receptor for the substrate, so that β-glucosylthioureidocalixarenes resulted[6,8] able to interact with Concanavalin A, on the contrary known as lectin selective for natural α-manno- and α-glucosides.

On the basis of these data that make glycosylthioureidocalixarenes an interesting class of selective multivalent ligands, and focusing on the *cone* calix[4]arene as scaffold, we decided to investigate from a conformational point of view two glycoclusters (**1** and **2**) both exposing mannosyl moieties but differing for the configuration at the anomeric position. Mannose is a relevant monosaccharide in biology, then these clusters could be in the future synthesized and studied as inhibitor of lectins involved in important processes. Actually, cluster **1** with the α-anomeric configuration has been recently reported in literature for decorating gold nanoparticles.[11] On the contrary, to the best of our knowledge, thioureidocalix[4]arene **2** containing β-mannosyl moieties has never been synthesized. In a sort of predictive challenge, in this investigation the two potential multivalent ligands have been compared in order to get more insights into the effects of the anomeric configuration of the sugar on the presentation mode of the glycosyl portion of glycoclusters.

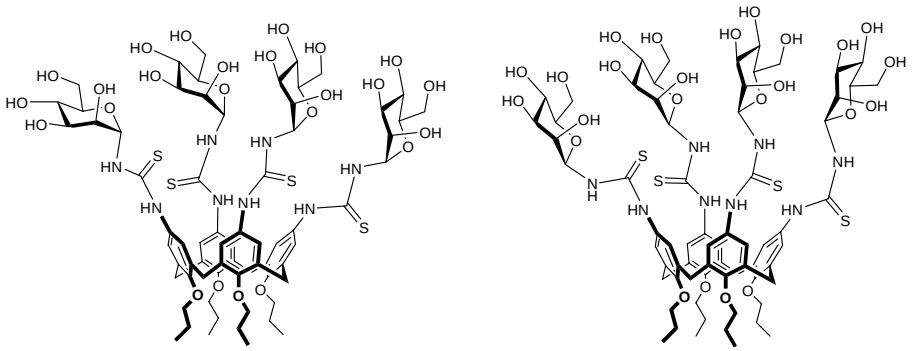

Chart 1

Thus, we have undertaken an in-depth theoretical study of α- and β-D-mannosylthioureido calix[4]arenes **1** and **2** (Chart 1) and, following our usual approach to dissect the problem in all its components, we have faced step by step the several computational items involved in the study: the choice of the suitable level of calculation; the evaluation of the properties of each monomeric component of calixarenes **1** and **2**; the need to deepen the knowledge of the intrinsic conformational properties of *cone*-calix[4]arenes with orientable groups at the upper rim; just at the end, the modeling the whole macrocycles **1** and **2** including their chiral mannosyl moieties.

Results and discussion.

Choice of the computational method

In a modeling study, the choice of the computational approach is of utmost importance for a correct description of the system. In the framework of the widespreadly used density functional theory, attention was focused on the standard B3LYP/6-31G(d) level[12,13] as the big molecular size of **1** and **2** did not allow the use of higher theory levels, that would cause unreasonably longer computational time. The first goal was to verify the suitability of this approach in correctly describing the different functionalities in the molecules, *i.e.* the thioureido group and the glycosyls. In the thioureido units the restricted rotation of the pseudo-amide NH-C=S bonds and the consequent tendency to planarity allow the existence of the four geometrical isomers designable as

ZZ, *ZE*, *EZ*, and *EE*. An extensive MP2/aug-cc-pVDZ study[14] of alkyl- and phenyl-substituted thiourea derivatives showed that conformations with alkyl groups *Z* to the sulfur atom are more stable by 0.4-1.5 kcal/mol than the *E* forms. In contrast, analysis of phenylthiourea revealed that in this case the opposite *E* isomer is preferred by 2.65 kcal/mol.

In compounds **1** and **2** the substituents at the two sides of thiourea are a propoxyphenyl and a glycosyl. Whereas for the propoxyphenyl it can be reasonably assumed a clear preference for the *E* geometry, as for the phenyl group, the glycosylthiourea conformational preferences have to be investigated. To the best of our knowledge, no calculations at the MP2 level of theory have been performed on glycosylthioureas. So, we decided to model at this level the simplified structures **3** and **4** (Chart 2). They present a thiourea at the anomeric position respectively in the α or β orientation and an axially oriented hydroxyl group at position 2 of a pyranose ring in the $^4C_1$ conformation, maintaining the main structural features required for a correct description of the mannosyl/thiourea interaction.

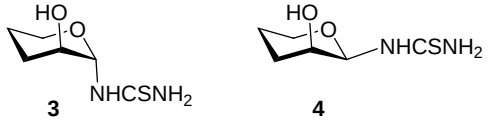

Chart 2

The *E* and *Z* geometries of compounds **3** and **4** were built and optimized at the MP2/aug-cc-pVDZ level. Table 1 reports the relative energy of the optimized structures. In both cases the *E* geometry is preferred over the *Z* one. Then we tested the DFT B3LYP functional, using the 6-31G(d) basis set, for its ability to reproduce the MP2 stability data; thus, we optimized in vacuum, at this level of theory, the couple of *E*/*Z* isomers of thioureas **3**-**4** as well as phenylthiourea (Table 1). The DFT approach was able to reproduce the greater stability of the *E* isomer of the three computed *N*-substituted-thioureas with an even greater energy difference than that computed at the MP2 level. Moreover, considering that vacuum optimization on glycosyl compounds might be

biased by the excessive strength of the hydrogen bonds involving the hydroxyl groups, the structures were optimized again taking into consideration the solvent effect by using a polarizable continuum model (PCM)[15-17] and choosing water as the solvent. Once more, the *E* isomers resulted more stable, though the values of the relative energy of the *Z* isomers were smaller than in the *in vacuum* optimizations. It is worth pointing out that the DFT approach combined with the solvent effect gives results comparable with those obtained with the MP2 approach in a much shorter computational time. Thus, throughout the present paper, all calculations were performed at the B3LYP/6-31G(d) level through optimizations in the PCM solvent model of water.

Table 1. Relative energy (kcal/mol) of the *E* and *Z* geometries of compounds 3 and 4 optimized at different levels of theory.

	MP2/aug-cc-pVDZ	B3LYP/6-31G(d)	B3LYP/6-31G(d)[a]
E-**3**	0.00	0.00	0.00
Z-**3**	6.35	7.23	3.42
E-**4**	0.00	0.00	0.00
Z-**4**	1.53	2.30	1.57
E- Phenylthiourea	0.00[b]	0.00	0.00
Z-Phenylthiourea	2.65[b]	3.92	2.54

[a] Optimization performed in a polarizable continuum solvent model (PCM) choosing water as the solvent. [b] Data from ref. 14.

Modeling of the monomers 5 and 6

In a stepwise approach to the study of the entire calixarenes, the conformational behavior of the single model monomeric α- and β-D-mannosylthioureas **5** and **6** (Chart 3) was investigated and the results are reported in Table 2. The aryl and the glycosyl groups on the two sides of thiourea should have, as discussed above, a defined preference for the *E* geometry at the respective pseudo-amide NH-C=S bond. Indeed, the *EE* geometry suffers from a severe steric strain that makes it the least stable isomer as indicated by the data in Table 2 for **5** and **6**. The balance between steric and stereoelectronic factors makes the *ZE* geometry preferred by the α-isomer **5** and the *EZ* by its β-anomer **6** whereas the *ZZ* geometry was found to be less stable than the global minimum by about 3 kcal/mol in both compounds.

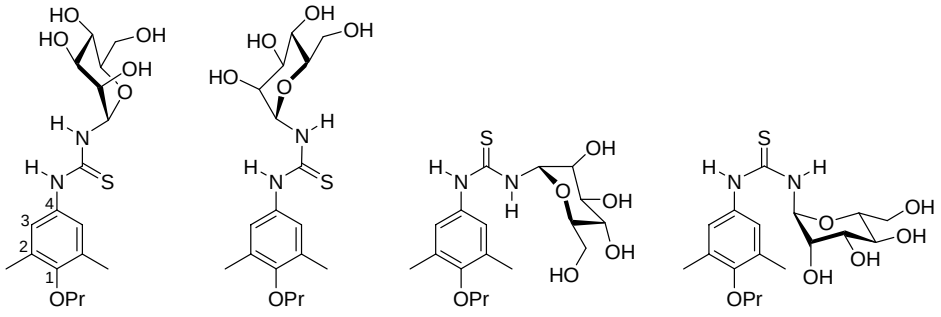

5-*ZZ* **5**-*ZE* **5**-*EZ* **5**-*EE*

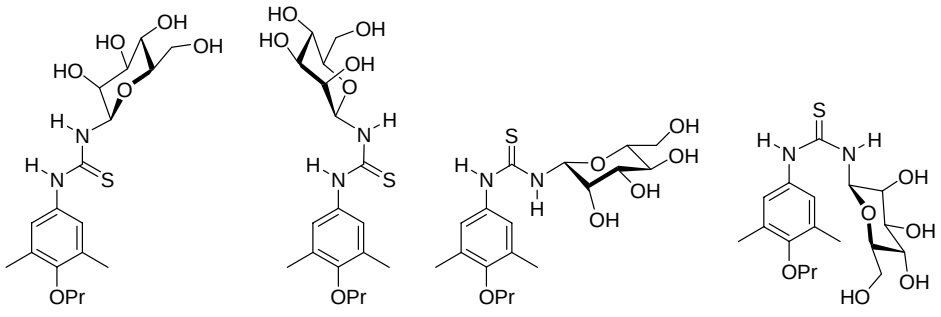

6-*ZZ* **6**-*ZE* **6**-*EZ* **6**-*EE*

Chart 3

Table 2. Relative energy (kcal/mol) of the four geometrical isomers of compounds 5 and 6 optimized at the B3LYP/6-31G(d) level in a water continuum solvent model.

	ZZ-a	*ZE-a*	*EZ-a*	*EE-a*	*ZZ-b*	*ZE-b*	*EZ-b*	*EE-b*
5	3.48	0.00	0.56	7.31	3.48	0.80	0.66	4.77
6	2.84	[a]	0.00	4.36	2.84	0.95	0.02	4.98

[a] Minimum not located. It converges to the *ZE-b* conformer during the optimization.

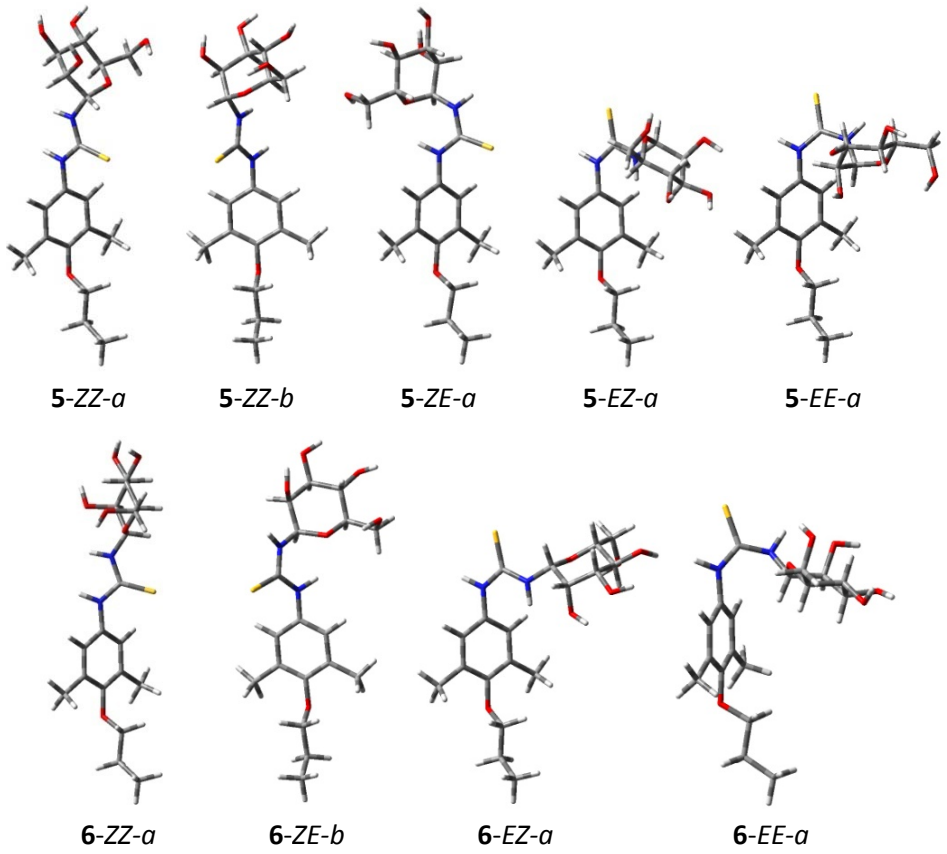

Figure 1. Three-dimensional plot of the *ZZ*, *ZE*, *EZ*, *EE* conformers of monomeric α- and β-D-mannosylthioureas **5** and **6**.

The three-dimensional plots reported in Figure 1 show that the *ZZ* and *ZE* geometries determine an almost extended shape for the molecules that, on the contrary, assume a bent shape in the *EZ* and *EE* geometries; in the latter ones the steric strain between the sugar and the phenyl ring is released by deviation of thiourea from planarity. Moreover, due to conjugation, there is the tendency of thiourea and phenyl to coplanarity; this tendency is hindered by the interactions of the phenyl *meta*-hydrogens with the NH hydrogen or the CS sulfur atoms that lead to a plane between the two groups of about 50-60°. Thus, for each thiourea geometry, there are two possible orientations with respect to phenyl that are not isoenergetic, due to the chirality of the monosaccharide. They are distinguished by the descriptors *a* and *b* in Table 2 and Figure 1, assigned on the basis of the dihedral angle τ_1, defined by the atoms C3-C4-N-C(=S) (Chart 3), with *a* used for $90° < \tau_1 < 270°$ and *b* for $-90° < \tau_1 < 90°$.

The symmetry properties of cone-calix[4]arenes substituted at the upper rim

When four propoxy groups are present at the lower rim of calix[4]arenes, as in the case of **1** and **2**, the macrocycle is locked in specific conformations, named by Gutsche[18] as *cone*, partial *cone*, 1,3-alternate, and 1,2-alternate, differing for the orientation of the phenyl groups. In the *cone* conformation the four aryl groups are oriented in the same direction originating a geometry usually represented as a C_4 symmetrical structure that, however, does not correspond to the true minimum energy structure. Actually, two opposite phenyl groups face each other at a distance much shorter than the other two thus making these macrocycles C_2 symmetrical structures. However, an easy equilibrium, in which the farther groups have approached and the closer ones have moved away, interchanges the close and the far phenyl groups making them indistinguishable.[19] This equilibrium, that could be called *breathing equilibrium*, can be schematically represented using rectangular shaped drawings in which the macrocycle is seen from a top view (Figure 2, **X** ⇆ **Y** equilibrium).

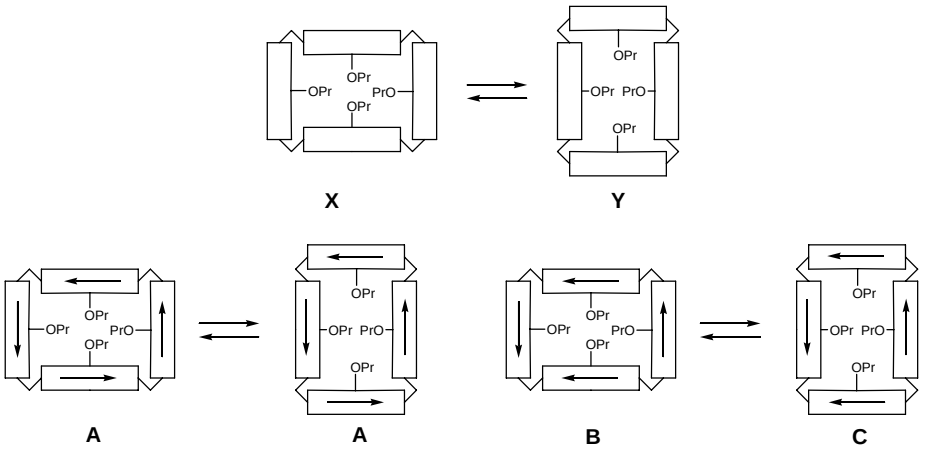

Figure 2. Schematic representation of the *breathing equilibrium* of *cone*-calix[4]arenes without (**X**, **Y**) and with (**A**, **B**, **C**) orientable groups at the upper rim.

The **X** and **Y** structures are indistinguishable but, when at the upper rim of calixarene are introduced groups that may assume two different orientations with respect to the phenyl rings, as for example the thiourea groups, a series of distinguishable conformers can exist. In Figure 2 the orientable groups are represented as arrows that can be arranged in combinations such as those indicated as **A**-**C** in Figure 2. The *breathing equilibrium* on these structures may produce a conformer indistinguishable from the starting one, as in the case of **A**, or a distinct conformer, as in the **B** ⇆ **C** equilibrium. A total of ten different combinations do exist; these ten conformers, **A**-**J**, are drawn in a simpler, more schematic, way in Figure 3. The conformers can interconvert through the *breathing equilibrium* (**B**/**C**, **D**/**G**, **E**/**F**, **H**/**I**) or through the rotation of an orientable group (arrow) with respect to the phenyl group to which it is linked. For example, **A** can be converted into **B** or **C** through the rotation of just one arrow; in turn, **B** can be converted into **D**, **E**, or **G**, and so on. These transformation can be represented by a graph (Figure 4) in which each solid line connects conformers interchangeable through rotation of an arrow and the dashed lines connect conformers interchangeable through the *breathing equilibrium*. At the two extremes are the counterclockwise (**A**) and clockwise (**J**) arrow arrangements that obviously require four *arrow rotations* to be converted one into the other.

All of the **A**-**J** geometries are chiral. Moreover, they can be grouped into five enantiomeric couples: **A** and **J**, **B** and **I**, **C** and **H**, **D** and **G**, **E** and **F**, *i.e.* all the couples at the opposite vertices of the graph of Figure 4 are enantiomerically related and hence isoenergetic. When the orientable groups contain chiral elements, all of the **A**-**J** geometries become diastereoisomeric so that the stability of all of them becomes different.

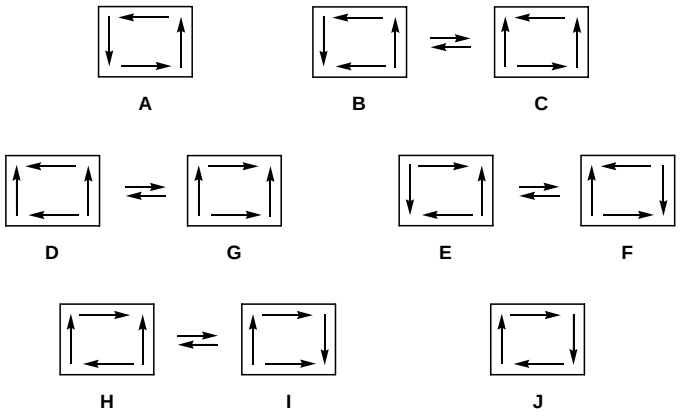

Figure 3. Schematic representation of the ten **A**-**J** conformations of a *cone*-calix[4]arene with four orientable groups at the upper rim.

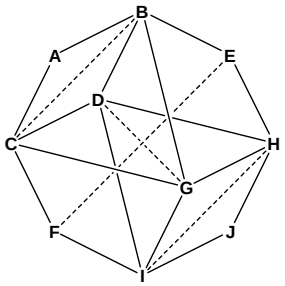

Figure 4. Graph representing the connections among the ten **A**-**J** conformations of a *cone*-calix[4]arene with four orientable groups at the upper rim through *arrow rotations* (solid lines) or *breathing equilibria* (dashed lines).

Modeling of the calixarenes 1 and 2

The complete structures of α- and β-D-mannosylthioureidocalix[4]arenes (**1** and **2**) was then built on the basis of the optimized monomeric structures **5** and **6** and taking into account the above discussed symmetry properties of *cone* calixarenes with orientable groups at the upper rim. The complete exploration of the conformational space of **1** and **2** through a systematic search approach may become very demanding. However, we decided to use this approach, instead of a molecular dynamics approach based on an empirical force field method, to guarantee an appropriate description of the different functionalities present in the molecules, in particular the thiourea groups. The procedure firstly exemplified for **1** was successively applied to compound **2**.

Thus, we built starting geometries for α-D-mannosylthioureidocalix[4]arenes **1** based on the energy minimum conformers of compound **5**, by selecting the *ZE* geometry for the thiourea and considering that the *ZE-a* and *ZE-b* geometries correspond, respectively, to the right- and left-oriented arrows in the schematic representations in Figure 3 when observed from a point of view external to the calix core. First of all, a geometry of **A** type was built, i.e. *ZE-a* geometries for the orientation of the four thiourea groups. It was optimized at the same calculation level used for the monomers obtaining the **1A**-*ZE* conformer reported in Figure 5.

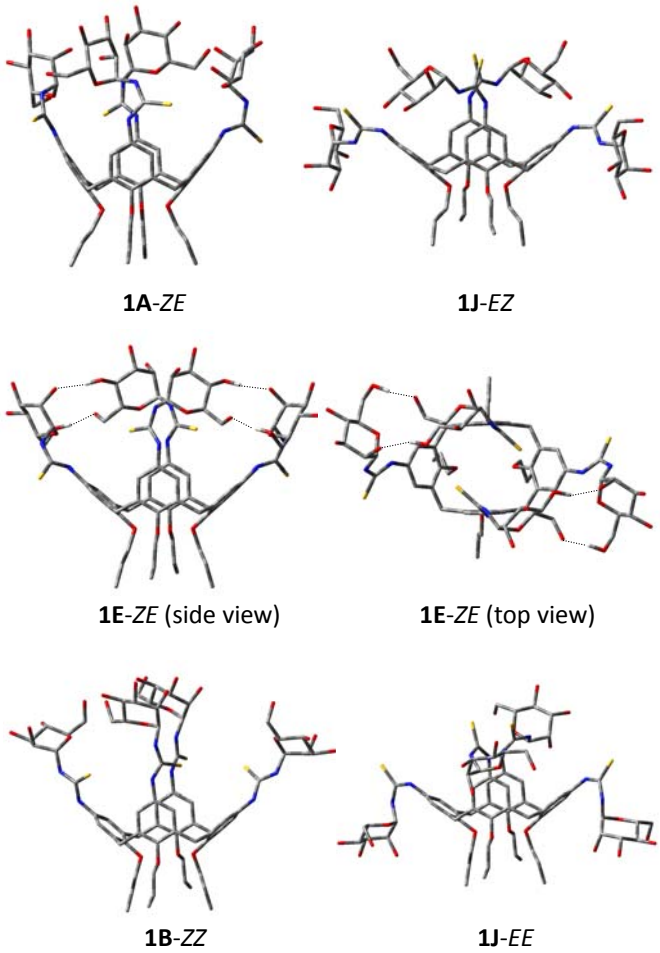

Figure 5. Three-dimensional plots of conformers **1A**-*ZE*, **1E**-*ZE*, **1J**-*EZ*, **1B**-*ZZ*, and **1J**-*EE* of α-D-mannosylthioureidocalix[4]arene **1**. The hydrogen atoms are omitted for clarity except those involved in the inter-residue H-bonds of **1E**-*ZE*.

From this conformer nine new starting geometries were built up, through suitable rotations of the thiourea groups with respect to the corresponding phenyl group (*arrow rotations*), and optimized. The relative energy of all the ten minimum energy conformers so obtained is reported in Table 1S (Supporting Information) together with the percentage populations at 298 K calculated through the Boltzmann equation. The global minimum, conformer **1E**-*ZE*, was largely preferred. In fact, the second and third conformers, **1C**-*ZE* and **1A**-*ZE*, were less stable by 3.09 and 4.43 kcal/mol, respectively, so that **1E**-*ZE* accounts for more than 99% of the overall population. Its three-dimensional plot is reported in Figure 5 whereas those of the other conformers are reported in

Figure 1S (Supporting Information). Conformer **1E**-*ZE* has a C_2 symmetrical geometry with adjacent couples of mannosyl residues interacting through hydrogen bonds. It is worthy pointing out that the four mannosyl residues are not equivalent, being identical each couple at the opposite sides of the molecule; in fact, two residues expose their β-face outward and the other two their α-face. As it can be seen from the graph in Figure 4, in order to interchange these two couple of residues, at least one *breathing equilibrium* and four *arrow rotations* are necessary, passing through four conformers of higher energy than **1E**-*ZE* (Scheme 1S, Supporting Information). So, the interchange of the two couples of residues should be rather difficult as a series of *arrow rotations* are necessary; moreover, these are much more difficult in **1E**-*ZE* than in monomer **5** as they require the breaking of the network of inter-residue hydrogen bonds.

Though the *ZE* orientation of the thiourea is preferred in the monomer **5**, it is necessary to ascertain that this conformational preference is maintained in **1**. Thus, the procedure above described for the *ZE* geometry was repeated for the other three thiourea geometries optimizing in each case the ten corresponding **A**-**J** conformations; the data of the preferred conformer for each thiourea geometry, **1J**-*EZ*, **1B**-*ZZ*, and **1J**-*EE*, are reported in Table 1S. All these geometries were shown to be much less stable than **1E**-*ZE*, being their relative energy, respectively, 9.19, 12.06, and 33.00 kcal/mol. Their three-dimensional plots are reported in Figure 5.

The approach used for the modeling of compound **1** was then applied to β-D-mannosylthioureidocalix[4]arene **2**, and the results are summarized in Table 2S and Figure 2S (Supporting Information). In this case a definite preference for the *EZ* geometry of the thiourea group was found and the global minimum conformer, accounting for almost 90% of the overall population, was shown to be **2A**-*EZ* (Figure 6) with the remaining 10% attributable to its **2G**-*EZ*, **2B**-*EZ*, and **2E**-*EZ* graph neighbors. The other thiourea geometries were shown to be less stable; in fact, the corresponding preferred **2I**-*ZE*, **2I**-*ZZ*, and **2A**-*EE* conformers showed relative energy values of 5.67, 8.84, and 25.56 kcal/mol, respectively. As for calixarene **1**, the global minimum conformer of calixarene **2**, **2A**-*EZ*, has a C_2 symmetrical geometry with two couples of identical

opposite β-mannosyl residues. However, it should be noted that in conformer **2A**-*EZ* these residues point outward with respect to the calix core so that no inter-residue hydrogen bond can be established. This allows a certain degree of conformational mobility that makes the *arrow rotations* easier than in the case of the α-anomer. Moreover, the two couples of sugar residues can easily interconvert; in fact, the *breathing equilibrium* from **2A**-*EZ* yields an identical **A**-type geometry with interchanged mannose residues (Scheme 2S, Supporting Information) thus making actually indistinguishable the four sugar residues.

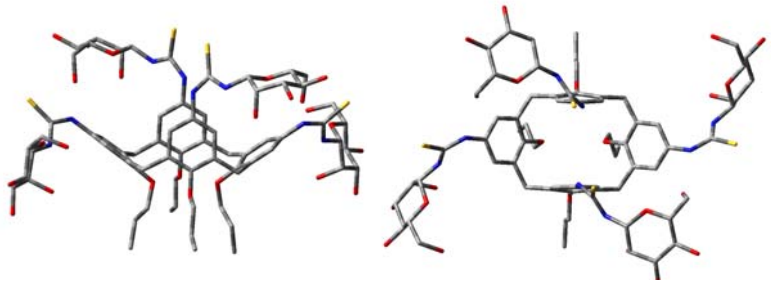

2A-*EZ* (side view) **2A**-*EZ* (top view)

Figure 6. Three-dimensional plots of the global minimum conformer **2A**-*EZ* of β-D-mannosylthioureido calix[4]arene **2**. The hydrogen atoms are omitted for clarity.

Conclusions

With the final goal to investigate the conformational properties of two α and β-mannosyl glycoclusters, and highlight their similarities and differences, we had to deal with the problem of the multiple arrangements allowed to *cone*-4-type calixarenes decorated with orientable groups at the upper rim. A systematic analysis of the possible orientations of these groups evidenced specific symmetry properties that can heavily influence the overall conformational behavior.

A restricted rotation around the bond connecting the phenyl groups of calixarenes to the functionality at their 4-position allows to define the substituent as an orientable group when this functionality is non-symmetric in its nature. The presence of orientable groups at the upper rim gives rise to ten different geometries schematically represented as **A**-**J** in Figure 3. These

geometries are chiral structures corresponding to five enantiomeric couples. Their interconversion relies onto two different processes, the *breathing equilibrium* and the *arrow rotation*. Depending on the extent of conjugation of the orientable group with the phenyl and the possibility for the groups decorating the calixarene structure to establish through space interaction such as hydrogen bonds, the ten **A**-**J** geometries are more or less easily interconvertible.

The theoretical study of α- and β-D-mannosylthioureidocalix[4]arenes **1** and **2** evidenced a huge difference in their conformational behavior that heavily influences the presentation mode of the saccharidic moieties. The preference of **1** for the *ZE* geometry of thiourea determines an extended shape of each monomeric unit. This allows the formation of hydrogen bonds between adjacent couples of mannosyl residues. The optimal orientation of these residues corresponds to that defined by the **E**-type geometry in which hydrogen bonds are established among the hydroxyl groups at positions 4 and 6 of one residue and those at positions 6 and 2 of the other one. Moreover, the residues expose alternatively their α or β face outward and, consequently, the four mannosyl residues are not equivalent. The β-isomer **2**, conversely, shows a neat preference for the *EZ* geometry of thiourea with a bent shape that turns the mannosyl residues away from the calixarene core preventing the formation of any inter-residue hydrogen bond. Consequently, **2** prefers the **A**-type geometry in which the four mannosyl residues are easily interchangeable simply through a *breathing equilibrium.*

In conclusion, though the two isomeric glycoclusters differ only in the anomeric configuration of the sugar, a great difference in their overall geometry has been evidenced so that a very different ability to interact with a protein partner can be hypothesized. This shows that the preliminary knowledge of the conformational properties of a calixarene glycocluster can become a powerful tool in driving the synthetic work towards the targets that are predicted to better fit the desired features for a useful multivalent presentation.

Computational Methods

All the calculations were carried out using the Gaussian09 program package.[20] All the structures were optimized at the B3LYP/6-31G(d) level[12,13] in the water solvent simulated using a self-consistent reaction field (SCRF) method, based on the polarizable continuum solvent model a polarizable continuum solvent model (PCM).[15-17]

Acknowledgments

The Italian Ministry of University and Research (PRIN 2010-11 grant, prot. 2010JMAZML, Italian network for the development of multivalent nanosystems) is gratefully acknowledged for financial support. CINECA is also acknowledged for the allocation of computer time.

Supporting Information Available: Schemes 1S and 2S, Tables 1S and 2S, Figures 1S and 2S, and electronic energy and Cartesian coordinates of all computed structures. This material is available free of charge via the Internet at http://pubs.acs.org.

References

1. Sansone, F.; Baldini, L.; Casnati, A.; Ungaro, R. *New J. Chem.* **2010**, *34*, 2715-2728.
2. Sansone, F.; Casnati, A. *Chem. Soc. Rev.* **2013**, *42*, 4623-4639.
3. Dondoni, A.; Marra, A. *Chem. Rev.* **2010**, *110*, 4949-4977.
4. André, S.; Sansone, F.; Kaltner, H.; Casnati, A;. Kopitz, J.; Gabius, H.-J.; Ungaro, R. *ChemBioChem* **2008**, *9*, 1649-1661.
5. André, S.; Grandjean, C.; Gautier, F.-M.; Bernardi, S.; Sansone, F.; Gabius, H.-J.; Ungaro, R. *Chem. Commun.* **2011**, *47*, 6126-6128.
6. Sansone, F.; Chierici, E.; Casnati, A.; Ungaro, R. *Org. Biomol. Chem.* **2003**, *1*, 1802-1809.
7. Torvinen, M.; Neitola, R.; Sansone, F.; Baldini, L.; Ungaro, R.; Casnati, A.; Vainiotalo, P.; Kalenius, E. *Org. Biomol. Chem.* **2010**, *8*, 906-915.

8. Sansone, F.; Baldini, L.; Casnati, A.; Ungaro, R. *Supramol. Chem.* **2008**, *20*, 161-168.
9. Consoli, G. M. L. ; Cunsolo, F.; Geraci, C.; Mecca, T.; Neri, P. *Tetrahedron Lett.* **2003**, 7467-7470.
10. Consoli, G. M. L.; Cunsolo, F.; Geraci, C.; Sgarlata, V. *Org. Lett.* **2004**, *6*, 4163-4166.
11. Avvakumova, S.; Fezzardi, P.; Pandolfi, L.; Colombo, M.; Sansone, F.; Casnati, A.; Prosperi, D. *Chem. Commun.* **2014**, *50*, 11029-11032.
12. Becke, A. D. *J. Chem. Phys.* **1993**, *98*, 5648-5652.
13. Lee, C.; Yang, W.; Parr, R. G. *Phys. Rev. B* **1988**, *37*, 785-789.
14. Bryantsev, V. S.; Hay, B. P. *J. Phys. Chem. A* **2006**, *110*, 4678-4688.
15. Cancés, E.; Mennucci, B.; Tomasi, J. *J. Chem. Phys.* **1997**, *107*, 3032-3042.
16. Cossi, M.; Barone, V.; Cammi, R.; Tomasi, *J. Chem. Phys. Lett.* **1996**, *255*, 327-335.
17. Barone, V.; Cossi, M.; Tomasi, J. *J. Comput. Chem.* **1998**, *19*, 404-417.
18. *Calixarenes: An Introduction;* C. D. Gutsche, Ed.; J. F. Stoddart, The Royal Society of Chemistry: Cambridge, 2008, p. 276.
19. Arduini, A.; Fabbi, M.; Mantovani, M.; Mirone, L.; Pochini, A.; Secchi, A.; Ungaro, R. *J. Org. Chem.* **1995**, *60*, 1454-1457.
20. Frisch, M. J.; Trucks, G. W.; Schlegel, H. B.; Scuseria, G. E.; Robb, M. A.; Cheeseman, J. R.; Scalmani, G.; Barone, V.; Mennucci, B.; Petersson, G. A.; Nakatsuji, H.; Caricato, M.; Li, X.; Hratchian, H. P.; Izmaylov, A. F.; Bloino, J.; Zheng, G.; Sonnenberg, J. L.; Hada, M.; Ehara, M.; Toyota, K.; Fukuda, R.; Hasegawa, J.; Ishida, M.; Nakajima, T.; Honda, Y.; Kitao, O.; Nakai, H.; Vreven, T.; Montgomery, J. A., Jr.; Peralta, J. E.; Ogliaro, F.; Bearpark, M.; Heyd, J. J.; Brothers, E.; Kudin, K. N.; Staroverov, V. N.; Keith, T.; Kobayashi, R.; Normand, J.; Raghavachari, K.; Rendell, A.; Burant, J. C.; Iyengar, S. S.; Tomasi, J.; Cossi, M.; Rega, N.; Millam, J. M.; Klene, M.; Knox, J. E.; Cross, J. B.; Bakken, V.; Adamo, C.; Jaramillo, J.; Gomperts, R.; Stratmann, R. E.; Yazyev, O.; Austin, A. J.; Cammi, R.; Pomelli, C.; Ochterski, J. W.; Martin, R. L.; Morokuma, K.; Zakrzewski, V. G.;

Voth, G. A.; Salvador, P.; Dannenberg, J. J.; Dapprich, S.; Daniels, A. D.; Farkas, O.; Foresman, J. B.; Ortiz, J. V.; Cioslowski, J.; Fox, D. J. Gaussian 09, Revision B.01; Gaussian, Inc., Wallingford, CT, 2010.